Tuning the interaction between spin-singlet and spin-triplet states of double donors with stress

K. Bergman, G. Grossmann, and H. G. Grimmeiss
Department of Solid State Physics, University of Lund, Box 118, S-221 00 Lund, Sweden

M. Stavola
AT&T Bell Laboratories, Murray Hill, New Jersey 07974

C. Holm and P. Wagner
Wacker Heliotronic GmbH, Postfach 11 29, D-8263 Burghausen, Federal Republic of Germany
(Received 20 July 1987; revised manuscript received 20 January 1988)

The interaction of the spin-singlet and spin-triplet terms of the $1s(A_1)1s(T_2)$ configuration under uniaxial stress, previously reported for Si:Se^0, is studied for Si:Te^0 where the spin-orbit interaction is much larger. For Si:Te^0 spin-triplet states are already observable at zero stress. Thus the range of stress values for which triplet states are seen and the number of observed states are greatly increased. The new data strongly confirm the model proposed for Si:Se^0. Furthermore, features not predicted by the previous model are tentatively assigned to the spin-triplet terms of the $1s(A_1)1s(E)$ configuration.

I. INTRODUCTION

In a recent Letter[1] on the neutral isolated selenium impurity in silicon (Si:Se^0), certain features in the absorption spectra of this double donor under uniaxial stress were interpreted as arising from a mixing of spin-singlet and spin-triplet states, which are coupled by the spin-orbit (s.o.) interaction. Preliminary results were also reported for Si:Te^0. In the present work, more heavily Te-doped samples have allowed us to investigate several new features due to spin-triplet states.

The well-known spin-singlet $1s$ states of the double donor Si:Te^0 are split by the valley-orbit interaction into A_1, E, and T_2 terms. The ground state is the $1s(A_1)^2$ configuration[5] with a binding energy of 1603 cm^{-1} [which is several times larger than the value 252 cm^{-1}, predicted by effective-mass theory (EMT) for a hydrogenlike center, or the value 452 cm^{-1}, which is an estimate within EMT of the ionization energy of a heliumlike system obtained by scaling atomic values]. Transitions from the ground state to the $1s(T_2)$ state give rise to an absorption line at 1288 cm^{-1} whose strength is due to the non-EMT character of the deep ground state. The binding energy of the $1s(E)$ state has been deduced to be 255 cm^{-1} from phonon-assisted Fano resonances.[6] Higher-lying excited states have binding energies in good agreement with the predictions of EMT.

The double donor is a two-electron system, and thus, in addition to the spin-singlet states, we expect every configuration to have spin-triplet states as well, except where prohibited by the Pauli principle, as is the case for the ground state. According to Hund's rule, the spin-triplet terms are expected to have higher binding energies than their spin-singlet counterparts due to the exchange interaction. Since the electric dipole operator cannot flip spins, optical transitions from the ground state to pure spin-triplet states are forbidden. The s.o. interaction splits the spin-triplet term into a multiplet, and may also mix equal-symmetry states of different spins if they are sufficiently close in energy. The s.o. interaction strength is proportional to the gradient of the electronic potential and thus stronger for orbitals where the electron penetrates the central cell, such as the $1s$ orbitals, than in more extended orbitals, such as the $2p$ orbitals.[7] Thus the $1s(T_2)$ orbital, which has the most penetrating orbital of all the excited states, is the most likely candidate for showing effects of mixing of spin-singlet and spin-triplet states. Because transitions to pure spin-triplet states are optically forbidden, it is the mixing with the singlet states that makes the triplets visible in our absorption experiments.

In our previous work on Si:Se^0, the s.o. interaction was too weak to mix the states sufficiently for the spin-triplet states[8] to be observed optically at zero stress. Stress was used to bring spin-singlet and spin-triplet states into near resonance to enhance their interaction. Thus, while a detailed study of a few spin-triplet states was possible, much of the complex level structure remained hidden.

Te is a more favorable case for the observation of triplet states because it is the heaviest of the chalcogens and thus has the largest s.o. coupling. An absorption to a triplet final state is observed already at zero stress. We show here detailed observations of several of the levels associated with the triplet multiplet under uniaxial stress, confirming the predictions of the model developed previously for the $1s(A_1)1s(T_2)$ configuration. Further, our new Te results show additional intriguing features which we speculate are due to components of the spin-triplet $1s(E)$ multiplet.

II. THEORETICAL MODEL

To understand the spectral data under uniaxial stress, we have developed a model of the $1s(A_1)1s(T_2)$ configuration. Since the $1s(T_2)$ orbital locally resembles a p state and the $1s(A_1)$ orbital an s state, the level structure becomes very similar to the $1s2p$ configuration of He I. In the following we assume that all two-electron states of the $1s(A_1)1s(T_2)$ configuration can be expanded in Slater determinants, which all contain the same two $1s(A_1)$ and $1s(T_2)$, orbitals.

In the absence of s.o. interaction, the exchange interaction splits the $1s(A_1)1s(T_2)$ configuration into a spin-singlet ($^1T_2$) and a spin-triplet ($^3T_2$) term, as shown in Fig. 1. The term splitting is determined by the parameter Δ_{ST}, which may be written as

$$\Delta_{ST}=2\left\langle 1s(A_1)(1)1s(T_2)(2)\left|\frac{e^2}{\epsilon\,|\mathbf{r}_1-\mathbf{r}_2|}\right|1s(T_2)(1)1s(A_1)(2)\right\rangle , \tag{1}$$

where ϵ is the dielectric function. As long as the s.o. coupling is negligible (as it is for Si:S^0 for example) the spin S remains a good quantum number and the triplet term cannot be detected in optical absorption because the ground state is a spin singlet.

The addition of a finite s.o. interaction splits the triplet term into A_2, T_2, and T_1+E levels, shown in Fig. 1. (We have neglected the possible small crystal-field splitting between E and T_1.) From symmetry consideration it follows (as shown in the Appendix) that the s.o. matrix elements within the $1s(A_1)1s(T_2)$ manifold may be parametrized in terms of only one parameter ξ, defined by

$$\xi=-2i\langle 1s(T_2,x)\,|\,V_y\,|\,1s(T_2,z)\rangle . \tag{2}$$

Here $1s(T_2,x)$ and $1s(T_2,z)$ are $1s(T_2)$ orbitals oriented along the x and z axes, and V_y is defined by the s.o. Hamiltonian:

$$H_{\text{s.o.}}=\sum_i \frac{\hbar}{2m^2c^2}(\nabla U\times\mathbf{p})_i\cdot\mathbf{s}_i=\sum_i \mathbf{V}_i\cdot\mathbf{s}_i . \tag{3}$$

In Eq. (2), ξ only depends on the p-like $1s(T_2)$ orbital, the s-like $1s(A_1)$ orbital does not contribute.

Due to the s.o. interaction, the T_2 levels deriving from the spin-singlet, $T_2(^1T_2)$, and from the spin-triplet, $T_2(^3T_2)$, are not longer pure spin states, and optical transitions to both states become allowed. We have assigned an absorption line at 1217 cm^{-1} of Si:Te^0 as transitions to the $T_2(^3T_2)$ level.[1] The terms from which the s.o. split states are primarily derived are given in parentheses.

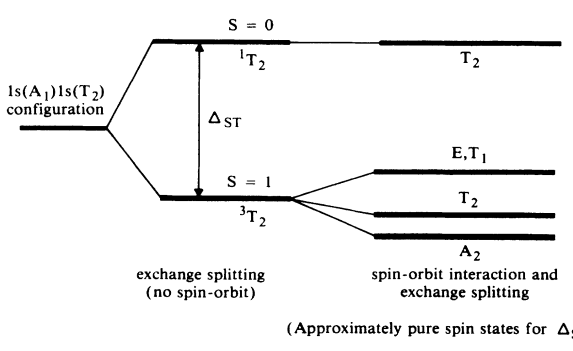

FIG. 1. Level diagram of the $1s(A_1)1s(T_2)$ configuration (T_d symmetry). The exchange interaction Δ_{ST} causes the configuration to split into the spin-singlet and spin-triplet terms. Turning on the spin-orbit interaction ξ splits the triplet term further. The levels are labeled by the appropriate irreducible representations of the T_d point group.

Here, as in our work on Si:Se^0, we use uniaxial stress to shift the spin-triplet and spin-singlet states into near resonance to enhance their mixing and study their interaction. The behavior of EMT-like states under uniaxial stress is accounted for by the deformation-potential approximation (DPA),[2,9,10] which describes the energy splittings and linear shifts of the conduction-band valleys. If we define δ as

$$\delta=\tfrac{1}{3}\Xi_u(s_{11}-s_{12})\,|\,T\,| , \tag{4}$$

then for a [001] compressional stress the valleys are split by 3δ, with the valleys along the z axis shifting towards lower energy by 2δ with respect to the center of gravity, and the x and y valleys shifting up in energy by δ. Here Ξ_u is the shear deformation potential, s_{11} and s_{12} are compliance tensor components, and T is the magnitude of the stress. (T is negative for a compression.) For [110] stress, the x and y valleys shift downwards by $\delta/2$, and the z valleys shift upwards by δ. For [111] stress the valleys do not split.

The valley-orbit interaction does not mix non-s states associated with different valleys, and hence these states split like the valleys. The s states, on the other hand, are made up of contributions associated with different valleys, and their stress dependence is more complicated. However, with knowledge of the symmetry-adapted linear combination coefficients of each state,[2] the stress dependence may be determined by adding the contribution from each valley, weighted by the coefficients squared. The effect of uniaxial stress is included in our model by assuming that all states, spin-singlet and spin-triplet, behave according to the DPA.

From, e.g., Griffith's tables,[11] we obtain coefficients for coupling of orbital T_2 wave functions with spin wave functions of A_1 ($S=0$) and T_1 ($S=1$) symmetry. In this basis, exchange, s.o., and DPA matrix elements can be evaluated in terms of Δ_{ST}, ξ, and δ, as discussed in the Appendix. (We assume that the envelope functions of the spin-singlet and spin-triplet terms are identical and independent of stress, insuring stress-independent values of ξ and Δ_{ST}.)

The s.o. coupling gives rise to non-zero off-diagonal elements in the Hamiltonian matrix between singlet and

triplet states, which make the triplet states visible already at zero stress for Te. Their effect is, however, dependent on the term splitting and greatly enhanced as stress shifts singlet and triplet components into near resonance. The Hamiltonian matrix is diagonalized to obtain the energy eigenvalues and the corresponding eigenvectors. From the eigenvectors the redistribution of oscillator strength among the interacting states may be calculated. (The oscillator strength is carried by the spin-singlet basis functions, and the eigenvectors give the amount of spin-singlet function in each eigenstate.) This analysis reproduces the general features of the avoided crossing behavior we observe in our experiments when the applied stress causes states to cross.

III. EXPERIMENTS

For this study Si epitaxial layers were grown using Te as a transporting agent.[3,12] The Te concentration was $\sim 5\times 10^{15}$ cm^{-3} in the Si epilayer. The 1-mm-thick layers were grown on floating-zone substrates to minimize the amount of interstitial oxygen in the samples; oxygen gives rise to an absorption band at 1205 cm^{-1} which might have interfered with an absorption band of interest which lies at 1217 cm^{-1} at zero stress. Samples for uniaxial-stress measurements were oriented and cut to dimensions of $2\times 2\times 7$ mm^3. Stress was applied along the long axis to end surfaces that had been ground flat and parallel.

The spectra were recorded at around 10 K using a Bomem DA3.02 series Fourier-transform spectrometer equipped with a Globar ir source, a Ge-on-KBr beam splitter and a $Hg_xCd_{1-x}Te$ detector. A commercial pneumatic cylinder was used to apply force to the center rod of a push-rod-type stress apparatus. The stress apparatus was mounted in a Leybold-Heraeus gas-flow cryostat and cooled by He contact gas. While the applied stress is well calibrated to the gas pressure used to drive the pneumatic cylinder, we have taken the $2p_0$ and $2p_\pm$ splittings as the measure of the stress in our numerical fits.

IV. RESULTS AND DISCUSSION

Figure 2(a) shows transmission spectra of Si:Te^0 for different values of [001] stress (which reduces the point group symmetry from T_d to D_{2d}). The two T_2 levels both split into two components which, for small stresses, shift as would be expected from the DPA. However, as the stress increases, components originating from each level approach each other, interact, and show avoided-crossing behavior. The other two components diverge for increasing stress, and the lowest component loses its intensity as the mixing due to the s.o. coupling gets weaker due to the increasing distance in energy between spin-singlet and triplet derived states.

Figure 2(b) shows the spectra for stresses along [110] (corresponding to the lower symmetry point group C_{2v}).

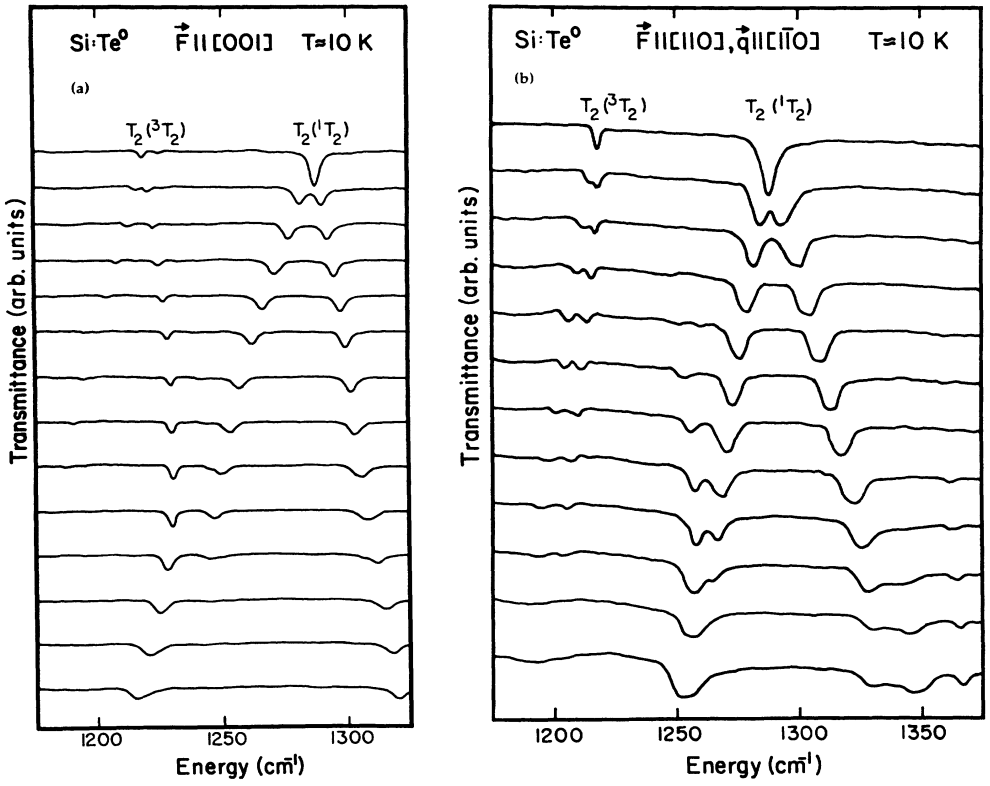

FIG. 2. Parts of transmission spectra of Si:Te^0 for different values of uniaxial stress. The spectra have been displaced downwards proportionally to stress. **F** is the applied force and **q** the propagation direction of the incident light. (a) **F**$\parallel$[001], (b) **F**$\parallel$[110].

The $T_2(^3T_2)$ state is again split, but both components initially visible at zero stress shift to lower energies. Here, a component of a state not visible in absorption at zero stress shifts upward to interact with $T_2(^1T_2)$ in an avoided crossing. A numerical fit of the model described above to our data is shown in Figs. 3(a) and 3(b). For simplicity we have omitted components of the spin-triplet term which are never expected to become visible in absorption. (A complete picture of the splitting diagram obtained from our model, including the omitted components, appears in Fig. 2 of Ref. 1.) The stress is measured in units of δ, defined above. δ has been obtained from the splitting of the $1s(A_1)\rightarrow 2p_{\pm}$ transition. This procedure reduces the uncertainty of our numerical fit due to errors in the stress. The fit has been made with three parameters: ξ, the s.o. coupling strength, Δ_{ST}, the exchange splitting of the spin-singlet and triplet terms in the absence of s.o. interaction, and a small linear shift of the ground state with stress.[13] From our numerical fit, we obtain the values $\xi = 13\ \text{cm}^{-1}$ and $\Delta_{ST} = 61\ \text{cm}^{-1}$.

The symmetries of states we have assigned in our model are given in Fig. 3. These assignments may be confirmed by polarized absorption measurements. Since the initial state of all transitions transforms as A_1, the polarization selection rules become simple; electric dipole transitions are only allowed to states which transform according to the same representation as the electric field vector of the incident light.

Figs. 4(a) and 4(b) show the effect of polarized light for fixed values of [001] and [110] stress. For [001] stress, i.e., D_{2d} symmetry, the electric field vector **E** transforms as B_2 for **E**$\|$**F** (**F** is the applied force) and as E for **E**$\perp$**F**. For [110] stress (C_{2v} symmetry) **E**$\|$[001] transforms as A_1 and **E**$\|$[110] as B_1 or B_2. The transitions allowed for each polarization direction are also indicated in Fig. 3. These expected polarization selection rules are confirmed by our experiments in detail.

V. ADDITIONAL SPECTRAL FEATURES AND TENTATIVE ASSIGNMENTS

Additional features, not accounted for by the model above are shown in Fig. 5. In the high-energy branch of the $T_2(^1T_2)$ state a complicated behavior is observed at the highest stresses. We see a crossing between three different components which are deduced to transform as A_1 in the C_{2v} point group from the polarization selection rules. Two of the spectral lines are visible over the whole stress range shown, but before they reach their point of closest approach, the lower line interacts with a third state over a short interval of stress.

Two lines can be identified with some certainty: The line shifting upward from low energy is of course a component of the $T_2(^1T_2)$. If one extrapolates the line with the highest energy linearly to zero stress, one arrives within a few cm^{-1} of the transition energy of the spin-singlet $1s(E)$ state which previously was derived from Fano resonance studies.[6] Similar crossings of $1s(T_2)$ and $1s(E)$ states have been observed[13] for Si:S^0 and Si:Se^0, although in a different region of stress because $1s(T_2)$ of

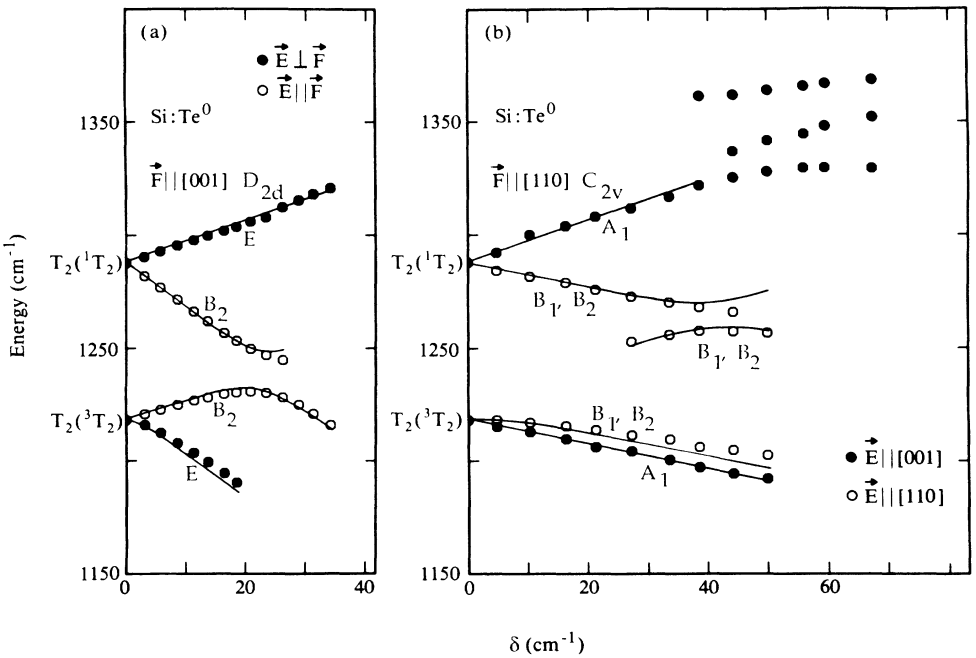

FIG. 3. Stress dependence of transition lines of Si:Te^0 due to transitions from the ground state to T_2 levels derived from the spin-singlet and spin-triplet terms of the $1s(A_1)1s(T_2)$ configuration. The stress is measured in units of δ, which has been obtained from the splitting of the $1s(A_1)\rightarrow 2p_{\pm}$ transition. The solid lines are given by a numerical fit to the data, and each component is labeled by the appropriate irreducible representation of the respective point groups (a) D_{2d} and (b) C_{2v}. For [110] stress, a complex behavior not predicted by our model is observed at stresses around $\delta = 50\ \text{cm}^{-1}$.

these defects is somewhat shallower. In Figs. 6(a) and 6(b) the expected stress-induced splitting of the $T_2(^1T_2)$ and $E(^1E)$ levels for [001] and [110] stresses are shown. Interaction is possible between components of the same symmetry, thus we only see a crossing for **F**||[110]. The assignment of the highest-energy line as a component of spin-singlet $1s(E)$ thus seems well founded. The shift rate under stress obtained from the linear extrapolation is, however, smaller than predicted by EMT and DPA. Thus an uncertainty remains when extrapolating data for higher stresses to zero stress.

The third line observed in Fig. 5 is unique to Te. The only member of the $1s$ manifold not yet accounted for is the spin-triplet $1s(E)$ term. Taking the direct product of E and the representation T_1, corresponding to $S=1$, one finds that ^3E is split into a $T_1(^3E)$ and a $T_2(^3E)$ level. However, the expectation values of the s.o. interaction for these states are zero. Only the matrix elements between the spin-triplet $1s(E)$ and $1s(T_2)$ terms cause the $T_1(^3E)$ and $T_2(^3E)$ to split. Under stress, the $T_2(^3E)$ level will split into E and B_2 in D_{2d} symmetry (**F**||[001]) and A_1, B_1, and B_2 in C_{2v} symmetry (**F**||[110]). The A_1 component of the $T_2(^3E)$ level is thus the only candidate within the $1s$ manifold for crossing for **F**||[110], as is indicated in Fig. 6 Because this line is only observed over a narrow stress region where it interacts with the upper $T_2(^1T_2)$ component, its zero stress value is difficult to determine. We assume its behavior under stress to be given by EMT and the DPA to find a $T_2(^3E)$ binding energy at zero stress about 8 cm^{-1} smaller than the $E(^1E)$. This analysis implies a violation of Hund's rule that contradicts our assignment. However, because of the large uncertainty in the extrapolation to zero stress, no definite statement can be made.

In D_{2d} symmetry the $T_2(^3E)$ level splits into B_2 and E, and we should observe a crossing of the E component of $T_2(^3E)$ in the high-energy branch of $T_2(^1T_2)$ (see Fig. 6). We have observed a shoulder on the spectral line in the high-energy branch of $T_2(^1T_2)$ in Fig. 2(a). This effect might support the interpretation of the extra line as a component of $T_2(^3E)$, but the effect is much weaker than that observed for **F**||[110].

VI. CONCLUSION

In conclusion, we have used uniaxial stress to study the spin-triplet $1s(T_2)$ manifold of the double donor Si:Te^0. The interaction between spin-singlet and spin-triplet

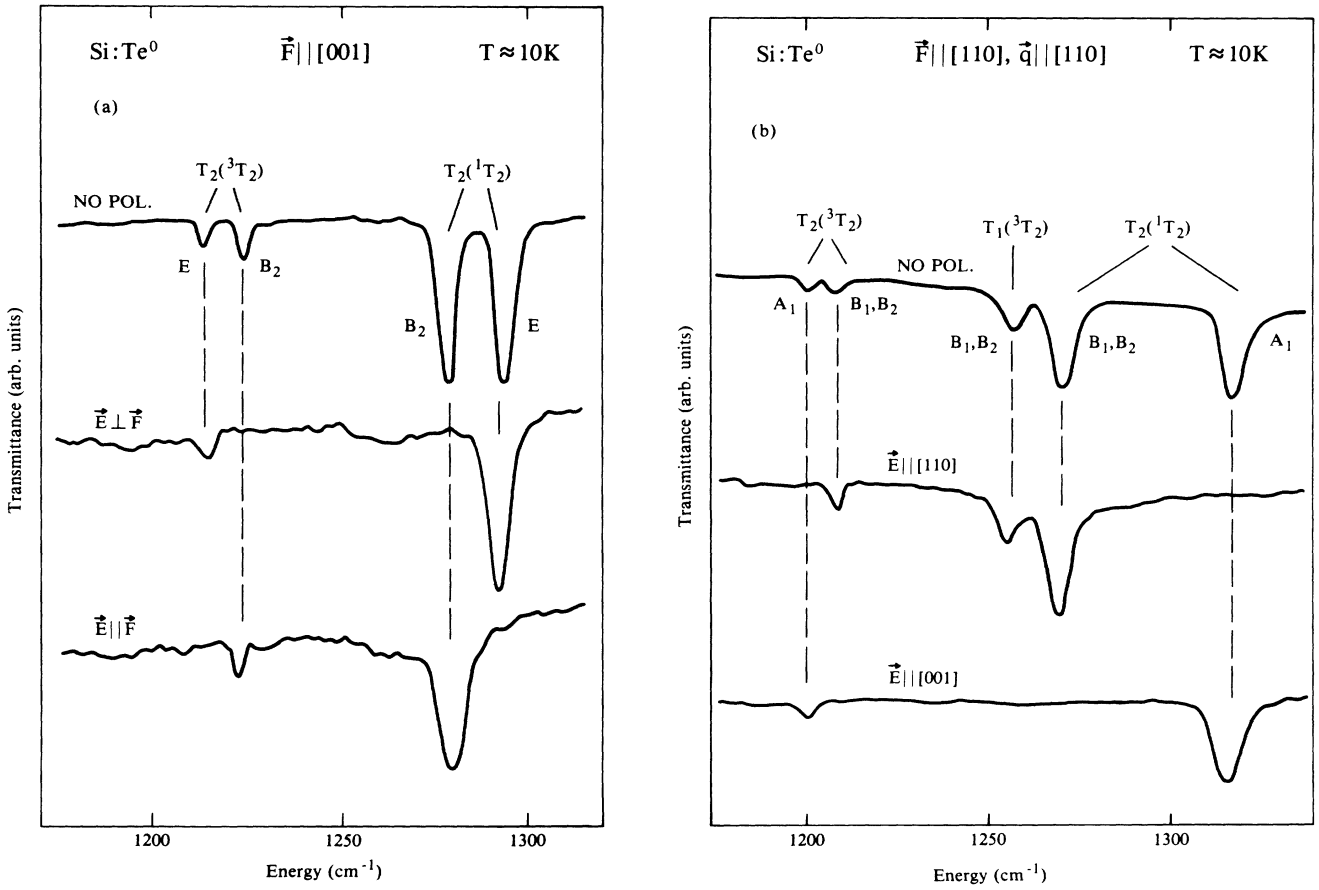

FIG. 4. Spectra recorded using polarized light at fixed values of uniaxial stress. The spectral components are labeled by their symmetry assignments according to our model. (a) [001] stress (D_{2d} symmetry), $T=25$ MPa; (b) [110] stress (C_{2v} symmetry), $T=153$ MPa. The polarization selection rules given by our model are confirmed in detail.

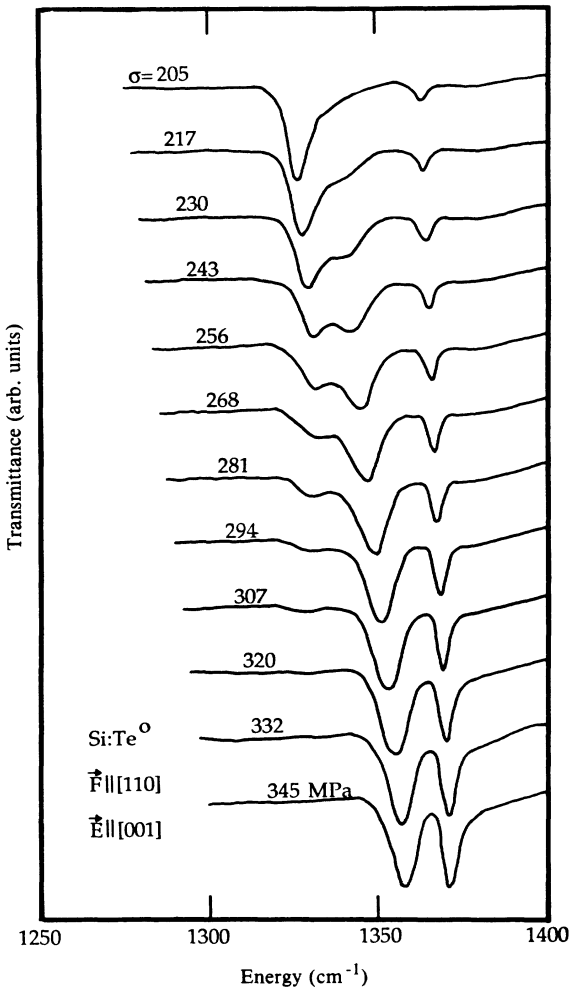

FIG. 5. Transmission spectra of Si:Te^0 for a series of values of [110] stress, showing avoided crossings between three different spectral components.

states is tuned with the uniaxial stress, thereby allowing weak triplet features at zero stress to be assigned and characterized. Furthermore, new triplet features are observed when their interaction with spin-singlet states is enhanced by near resonance. We find that the model we have developed provides an excellent account of the behavior of Si:Te^0 under stress where the spectral information is richer and more complex than in our previous study[1] of Si:Se^0. However, the numerical fit to the data is not as good for Si:Te^0 as for the Si:Se^0 case, which indicates that some of the assumptions (for example, simple DPA behavior of all levels) on which the model is based do not hold rigorously for Si:Te^0.

From our numerical fits for Si:Te here and for Si:Se in our previous work[1] we obtain the values $\xi=3.2$ cm^{-1} for Se and $\xi=13$ cm^{-1} for Te. The fact that we could not observe any singlet-triplet interaction for Si:S^0 has lead us to estimate ξ to be less than 2 cm^{-1} for this case. This trend in coupling strengths is consistent with our expectation that the heavier chalcogens should have larger s.o. coupling and is in reasonable agreement with the trend in atomic values.[14]

The many-electron contributions to the binding energies, a Δ_{ST} of 48.5 cm^{-1} for Si:Se and 61 cm^{-1} for Si:Te, correspond to significant fractions (19% and 24%, respectively) of the EMT $1s$ binding energy, 252 cm^{-1}. The slightly larger value for Te reflects the fact that the $T_2(^1T_2)$ state of Si:Te^0 is the deepest of all the neutral isolated chalcogen centers (the binding energy exceeds the EMT $1s$ value by 25%). This enhanced binding energy implies larger overlap of the $1s(A_1)$ and $1s(T_2)$ orbitals, and hence a larger exchange interaction. It is also an indication that EMT cannot fully describe this state, and hence one cannot expect the DPA to be entirely valid for this state either, leading to the less perfect numerical fits to our data that we have described above.

At higher stresses we observe a stress-shifted component of spin-singlet $1s(E)$, corroborating the assign-

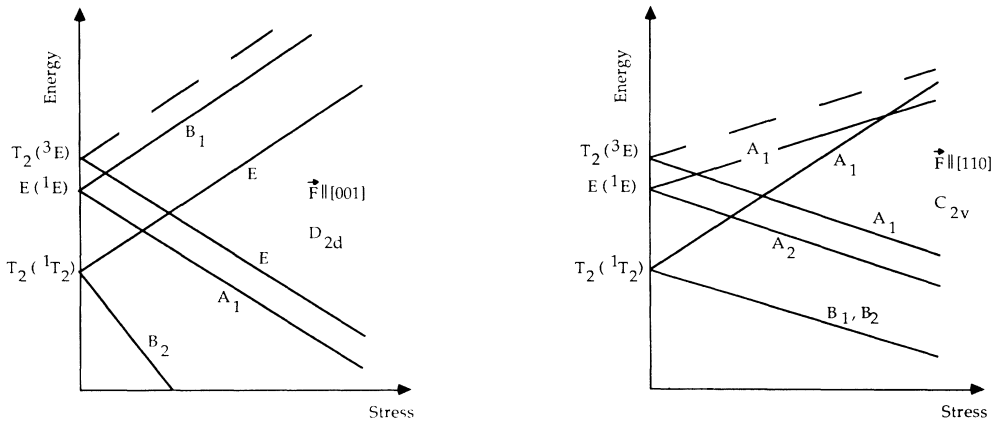

FIG. 6. Schematic diagram of the expected stress dependence of some $1s$ states of Si:Te^0. Components which may be relevant to the interpretation of the spectra in Fig. 5 have been labeled by the irreducible representations of the appropriate point group.

ment based on Fano resonances. An additional line is interpreted as a component of spin-triplet $1s(E)$, but uncertainties in the stress dependence prevent a detailed analysis.

Note added in proof. R. E. Peale *et al.* have recently made a study of the Zeeman splitting of chalcogen double donors in Se [this issue, Phys. Rev. B 37, 10 829 (1988)]. These authors find a s.o. coupling greater than reported here by a factor of ~ 2. They have also noted that the s.o. coupling between $^3T_2$ and $^1T_2$ terms might be different from that within $^3T_2$. (We have measured the former, Peale *et al.* the latter.) Possible support for this interpretation of the apparent discrepancy in the s.o.-coupling determinations comes from the data displayed in Fig. 3(b) here. G. Grossmann and F. S. Ham (unpublished) have independently noted that the fit to the components of $T_2(^3T_2)$ that shift downward would be improved by a value of the s.o. coupling that is larger than we have determined by fitting to the avoided crossing. This splitting of the downward shifting $T_2(^3T_2)$ components is due to the s.o. coupling within $^3T_2$ and might be expected to be in better agreement with the data of Peale *et al.* Further experiments will be required to establish these ideas.

ACKNOWLEDGMENTS

We are grateful for helpful discussions with E. Janzén and F. S. Ham and for the technical support of J. Henriksen. The work of M.S. was performed at the University of Lund, Sweden

APPENDIX

In the absence of s.o. interaction, i.e., for a spin-independent Hamiltonian, the eigenfunctions belonging to the $1s(A_1)1s(T_2)$ configuration can be written as products of spatial wave functions $|T_2,\mu\rangle$ and spin functions $|S,M_s\rangle$

$$|T_2S\mu M_s\rangle = |T_2,\mu\rangle\,|S,M_s\rangle ,$$

where $|T_2,\mu\rangle$ is symmetric (antisymmetric) under permutation for the spin-singlet (triplet). The spin functions transform as A_1 ($S=0$) and T_1 ($S=1$), and the transformation properties of the $|T_2,\mu\rangle$ states are, in analogy to angular momentum p functions, chosen as

$$|T_2,1\rangle \sim -\frac{i}{\sqrt{2}}(x+iy) ,$$

$$|T_2,0\rangle \sim iz ,$$

$$|T_2,-1\rangle \sim \frac{i}{\sqrt{2}}(x-iy) .$$

Expanding the s.o. Hamiltonian in spherical components,

$$H_{\text{s.o.}} = \sum_i \sum_\nu (-1)^\nu V_i^\nu s_i^{-\nu} ,$$

the s.o. matrix elements within the $^3T_2$ term ($S=1$) can be written as

$$\langle T_2S\mu M_s | H_{\text{s.o.}} | T_2S\mu' M_s'\rangle = \sum_i \sum_\nu (-1)^\nu \langle T_2\mu | V_i^\nu | T_2\mu'\rangle \langle SM_s | s_i^{-\nu} | SM_s'\rangle .$$

The operators V^ν and $s^{-\nu}$ transform according to T_1, and since the decomposition of $T_1\times T_2$ only contains T_2 once, it follows from the Wigner-Eckart theorem that

$$\langle T_2\mu | V_i^\nu | T_2\mu'\rangle = \langle T_2\mu | T_1T_2\nu\mu'\rangle \alpha_i ,$$

where α_i is a constant, independent of μ, ν, and μ', and where the coupling coefficients $\langle T_2\mu | T_1T_2\nu\mu'\rangle$ can be found in, e.g., Griffith's tables.[11] Similarly, as the states $|SM_s\rangle$ form a basis of T_1, we find

$$\langle SM_s | s_i^{-\nu} | SM_s'\rangle = \langle T_1M_s | T_1T_1-\nu M_s'\rangle \beta_i .$$

Summing over i we finally obtain

$$\langle T_2S\mu M_s | H_{\text{s.o.}} | T_2S\mu' M_s'\rangle = \xi \sum_\nu (-1)^\nu \langle T_2\mu | T_1T_2\nu\mu'\rangle \langle T_1M_s | T_1T_1-\nu M_s'\rangle , \tag{A1}$$

where thus all matrix elements within the $^3T_2$ manifold are expressed in terms of a single parameter ξ. This parameter may be determined by evaluating the matrix element in a particularly simple case. From Eq. (A1) we find, e.g.,

$$\langle T_2S11 | H_{\text{s.o.}} | T_2S11\rangle = \xi/2 .$$

On the other hand, assuming $|T_2S11\rangle$ to be given by a single Slater determinant of $1s(A_1)\uparrow$ and $1s(T_2,1)\uparrow$ orbitals, one can evaluate the matrix element in terms of these one-particle orbitals, whereby one may identify ξ as

$$\xi = -2i\langle 1s(T_2,x) | V_y | 1s(T_2,z)\rangle . \tag{A2}$$

From the decomposition of $T_2\times T_1$, one finds that the $^3T_2$ term splits into A_2, T_2, and (T_1+E) levels, where the parentheses indicate that T_1 and E are not split by $H_{\text{s.o.}}$. Using the coupling coefficients above, we can directly write down those linear combinations of the states $|T_2S\mu M_s\rangle$ that form basis functions of these representations, which diagonalize $H_{\text{s.o.}}$. Evaluating the expectations values of $H_{\text{s.o.}}$ in this basis using Eq. (A1), one finds that A_2 shifts by $-\xi$, T_2 by $-\xi/2$, and (T_1+E) by $\xi/2$. The resulting multiplet splitting pattern thus agrees with that of $1s2p\ ^3P$ of He I.

Apart from the multiplet splitting of $^3T_2$, $H_{\text{s.o.}}$ also introduces a coupling between $T_2(^1T_2)$ and $T_2(^3T_2)$. We have, e.g.,

$$\langle T_2,0(^1T_2) | H_{\text{s.o.}} | T_2,0(^3T_2)\rangle = \langle T_2,0(^1T_2) | H_{\text{s.o.}} | \frac{1}{\sqrt{2}}(|T_2T_1-11\rangle - |T_2T_11-1\rangle) ,$$

where we have used the coupling coefficients above to expand the $|T_2,0(^3T_2)\rangle$ state. If we again approximate $|T_2,0(^1T_2)\rangle$ and the spin-triplet states $|T_2T_1\mu M_s\rangle$ by Slater determinants and take the $1s(A_1)$ and $1s(T_2)$ orbitals of the spin-singlet and the spin-triplet to be the same, the coupling matrix element is found to be $\xi/\sqrt{2}$, where ξ again is given by Eq. (A2).

To determine the matrix elements of the stress perturbation H_{stress}, we note that H_{stress} is diagonal in the basis $|T_2S\mu M_s\rangle$ for stress applied along [110] or [001],

$$\langle T_2S\mu M_s | H_{\text{stress}} | T_2S'\mu'M_s'\rangle = \langle T_2,\mu | H_{\text{stress}} | T_2,\mu\rangle \delta_{S,S'}\delta_{M_s,M_s'}\delta_{\mu,\mu'} \quad \text{(A3)}$$

For stress along [110], we have

$$\langle T_2,\pm 1 | H_{\text{stress}} | T_2,\pm 1\rangle = -\frac{\delta}{2} ,$$

$$\langle T_2,0 | H_{\text{stress}} | T_2,0\rangle = \delta ,$$

while for [001] stress,

$$\langle T_2,\pm 1 | H_{\text{stress}} | T_2,\pm 1\rangle = \delta ,$$

$$\langle T_2,0 | H_{\text{stress}} | T_2,0\rangle = -2\delta ,$$

where δ is given by Eq. (4). Evaluating matrix elements of H_{stress} in the basis that diagonalizes $H_{\text{s.o.}}$ within the triplet multiplet, H_{stress} is found to be almost diagonal. Only a few off-diagonal elements are nonzero, in addition to the singlet triplet coupling due to $H_{\text{s.o.}}$ found above. The secular problem thus reduces to a set of smaller ones, which at most are three dimensional.

[1] K. Bergman, G. Grossmann, H. G. Grimmeiss, and M. Stavola, Phys. Rev. Lett. **56**, 2827 (1986).

[2] A. K. Ramdas and S. Rodriguez, Rep. Prog. Phys. **44**, 1297 (1981).

[3] H. G. Grimmeiss, E. Janzén, H. Ennen, O. Schirmer, J. Schneider, R. Wörner, C. Holm, E. Sirtl, and P. Wagner, Phys. Rev. B **24**, 4571 (1981).

[4] The Mulliken notation used is taken from M. Tinkham, *Group Theory and Quantum Mechanics* (McGraw-Hill, New York, 1964).

[5] The neutral centers discussed in this paper are two-electron systems, and one should discuss the electronic structure in terms of configurations. However, since all excited configurations are one-electron excitations leaving one electron in the $1s(A_1)$ orbital, we will often follow common usage and refer to configurations such as $1s(A_1)1s(T_2)$ simply as the $1s(T_2)$ state.

[6] E. Janzén, G. Grossmann, R. Stedman, and H. G. Grimmeiss, Phys. Rev. B **31**, 8000 (1985).

[7] The contribution to the s.o. interaction from the light silicon atoms may be neglected compared to the contribution from the heavy chalcogen impurity atoms discussed here.

[8] The spin-orbit interaction mixes states with different spins, and only the total (pseudo-) angular momentum J remains a good quantum number. However, as long as the term separation is large compared to the s.o. coupling strength, S will approximately be a good quantum number.

[9] C. Herring, Bell System Tech. J. **34**, 237 (1954).

[10] C. Herring and E. Vogt, Phys. Rev. **101**, 944 (1955).

[11] J. S. Griffith, *The Theory of Transition Metal Ions* (Cambridge University Press, London, 1961).

[12] C. Holm and E. Sirtl, J. Cryst. Growth **54**, 253 (1981).

[13] K. Bergman, G. Grossmann, H. G. Grimmeiss, M. Stavola, and R. E. McMurray, Jr., in Ph.D. thesis of K. Bergman, University of Lund, 1987.

[14] F. Herman and S. Skillman, *Atomic Structure Calculations* (Prentice-Hall, Englewood Cliffs, NJ 1963).